JOC The Journal of Organic Chemistry

Note

pubs.acs.org/joc

Computational and DNMR Investigation of the Isomerism and Stereodynamics of the 2,2′-Binaphthalene-1,1′-diol Scaffold

Andrea Mazzanti,*[,†] Michel Chiarucci,[†] Keith W. Bentley,[‡] and Christian Wolf*[,‡]

[†]Department of Industrial Chemistry "Toso Montanari", University of Bologna, Viale Risorgimento 4, I-40136 Bologna, Italy

[‡]Department of Chemistry, Georgetown University, Washington, D.C. 20057, United States

Supporting Information

ABSTRACT: The relative stabilities of three conformational isomers of 2,2′-binaphthalene-1,1′-diol diisobutyrate and the energy barriers to rotation about the pivotal aryl−aryl bond and the two aryl−oxygen bonds were investigated by variable-temperature NMR spectroscopy in conjunction with DFT computations. The experimental and calculated data were found to be in very good agreement and provide new insights into the dynamic stereochemistry of BINOL-derived tropos ligands.

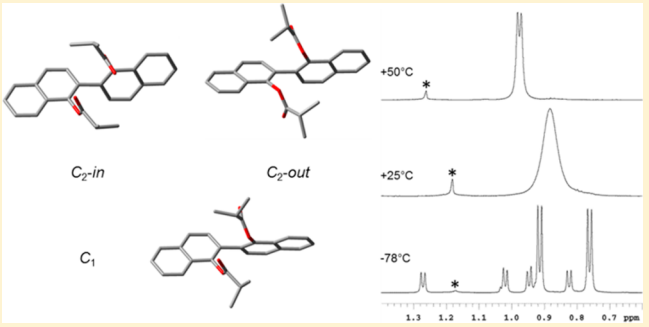

BINOL (1,1′-binaphthalene-2,2′-diol) is inarguably one of the most successful chiral ligands used in asymmetric synthesis.[1] The general usefulness of this important atropisomer has been attributed to its fairly rigid C_2-symmetric structure and its stability toward racemization even at high temperatures.[2] However, the properties of conformationally labile analogues of BINOL are not well understood, and the dynamic stereochemistry of 2,2′-binaphthalene-1,1′-diol (Figure 1) and other tropos ligands has received limited attention.

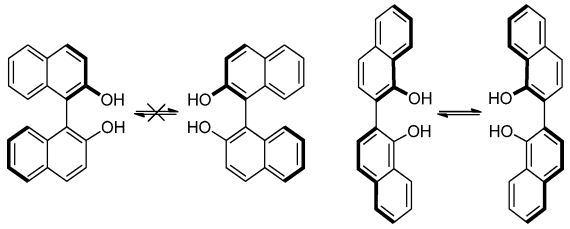

Figure 1. Structures of (left) conformationally stable BINOL and (right) rapidly racemizing 2,2′-binaphthalene-1,1′-diol.

A noticeable exception is the racemization kinetics of 2,2′-bis(diphenylphosphino)-1,1′-biphenyls (biphep ligands), which have been studied in detail by Trapp and others.[3]

To date, the unique combination of axial chirality and conformational flexibility of 2,2′-dihydroxybiphenyls and 2,2′-binaphthalene-1,1′-diols has led to several noteworthy applications, including amplification of chirality in liquid crystals,[4] circular dichroism chemosensing of chiral compounds,[5] and optimization of the efficiency of chiral catalysts.[6] We recently determined the rotational free energy barrier of 1,1′-biphenyl-2,2′-diol diisobutyrate by variable-temperature (VT) NMR spectroscopy to be $\Delta G^{\ddagger}$ = 12.6 kcal/mol, which corresponds well to the rotational barrier of 11.5 kcal/mol calculated by Fujimura for the corresponding free biphenol.[7] Following our previously reported protocol for the transformation of readily available 1-naphthol (**1**) into 2-bromo-1-methoxynaphthalene (**3**) and 1-methoxy-2-naphthylboronic acid (**4**), we prepared 2,2′-binaphthalene-1,1′-diol (**6**)[5e] and then obtained the diisobutyrate derivative **7**, which exists as a complex mixture of enantiomeric and diastereomeric conformers due to hindered rotation about the aryl−aryl axis and the two aryl−ester bonds (Scheme 1).

The racemization kinetics of numerous axially chiral biaryls have been investigated, and the steric and electronic effects of various ortho, meta, and para substituents on the rotational energy barrier are documented in the literature.[8] This is also the case for rotation about the chiral axis in aryl ketones, amides, sulfoxides, sulfones, esters, amides, amines, anilides, and derivatives thereof.[9] To our surprise, rotations about arene−oxygen bonds, in particular in aryl esters, has rarely been investigated. The stereochemistry and isomerization reaction of atropisomeric diaryl ethers has received notable attention because this motif is an important component in vancomycin and other biologically active compounds. Kessler et al.[10] calculated the free activation enthalpy for the rotation about the aryl−oxygen bond in a 2,6-diisopropylphenyl ether as 17.8 kcal/mol at 57 °C using the dynamic NMR (DNMR) coalescence method. Clayden found that the conformational isomers of diaryl ethers carrying at least three bulky ortho substituents are stable toward interconversion at room temperature.[11] Siddall's group was probably the first to observe rotational isomers of phenol esters under cryogenic conditions,

Received: March 4, 2014
Published: March 28, 2014

   dx.doi.org/10.1021/jo5005229 | J. Org. Chem. 2014, 79, 3725−3730

Scheme 1. Synthesis of 2,2′-Binaphthalene-1,1′-diol Diisobutyrate (7)

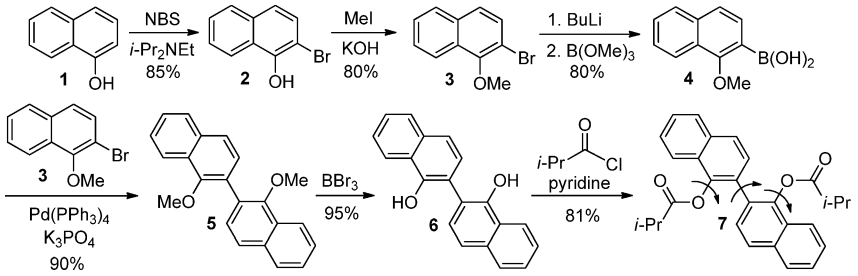

but they were not able to accurately determine the racemization kinetics.[12]

We realized that diester **7** provides a direct entry into investigations of both the aryl−aryl rotation of BINOL-derived tropos ligands and the rotation about aryl−ester bonds. The isopropyl groups were introduced to serve as NMR probes to analyze the axial chirality of the 2,2′-binaphthalene-1,1′-diol core.[13] In addition, rotation of the isobutyryl moieties about the aryl−oxygen axes was expected to give rise to several diastereomeric conformers. The ^{1}H NMR spectra of **7** taken at room temperature showed that the signal corresponding to the methyl moieties in the isopropyl groups was very broad. When the temperature was increased to 50 °C, the signal became a doublet. When the temperature was reduced below 25 °C, the signal split at about 10 °C into a broad doublet, and a complex line shape evolution was observed at lower temperatures. At −78 °C, at least six doublets with different intensities appeared (Figure S1 in the Supporting Information). The same unbalanced splitting was observed for the isopropyl CH moiety. The presence of such a number of signals cannot be related solely to the aryl−aryl rotation, which should produce only two diastereotopic doublets with the same intensity.

To account for the wealth of signals, a second conformational process yielding diastereoisomeric conformations must be considered. A preliminary scan of the potential energy surface (PES) was performed by means of a molecular mechanics approach (MMFF94 force field).[14] The best conformations found in a 10 kcal/mol window were subsequently optimized with DFT at the B3LYP/6-31G(d) level,[15] and frequency analysis confirmed that they corresponded to energy minima. Three clusters of conformations were found to be similar in energy. Within each cluster, the different dispositions of the isopropyl group with respect to the carbonyl group generate different conformations with very similar energies. Because of the bulkiness of the isopropyl group, the esters have the *Z* conformation in all of the optimized conformations, as is widely accepted.[16] Disregarding the conformational flexibility of the isopropyl groups, the main difference among the three conformational forms resides in the relative orientation of the isobutyrate moieties (Figure 2).

If the aryl−aryl axis perspective is considered, one conformation has the two carbonyls facing each other, in the second they point away, and in the third one carbonyl is close to the oxygen of the other ester moiety. The first two conformations belong to the C_2 symmetry point group, and they can conveniently be named as "C_2-*in*" and "C_2-*out*", respectively. The third conformation has C_1 symmetry. The calculated energies of the three conformations are enclosed in a 1 kcal/mol window, so all of them should be observable if the aryl−oxygen rotation is frozen. DFT calculations were also

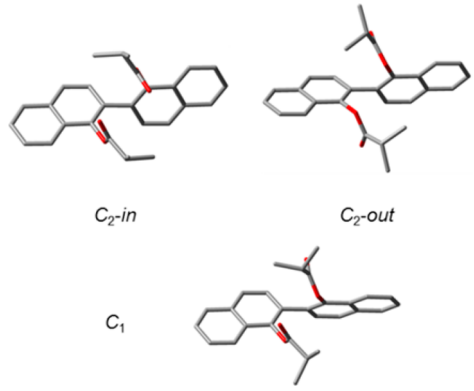

Figure 2. The three conformations of **7**. Hydrogens have been removed for clarity.

performed to find the transition states for the aryl−aryl rotation and for the aryl−OCOR rotation. The optimized transition state for the aryl−aryl rotation corresponds to a steric barrier with a planar geometry in which the two esters are on opposite sides with respect to the Ar−Ar axis (C_1−C_2−$C_{2'}$−$C_{1'}$ dihedral angle ≈ 180°). This TS is responsible for the enantiomerization and was found to be at 15.8 kcal/mol at the B3LYP/6-31G(d) level. The transition state for the rotation of one *i*-PrC(O)O group was found to be at 11.8 kcal/mol. It corresponds to a conformation where the carbonyl crosses the hydrogen at position 8 of naphthalene. The alternative transition state where the carbonyl unit points toward the second naphthalene is higher in energy by 1.4 kcal/mol (3D structures of the TS are shown in Figure S2 in the Supporting Information).

Being rather similar in energy, the two dynamic processes should occur within the same temperature range, providing three diastereoisomers (each one corresponding to an enantiomeric pair) when both of rotations are frozen. This interpretation could explain the evolution of the methyl line shape and the crowded spectrum at low temperature. Given the complexity of the ^{1}H NMR spectrum, we acquired VT ^{13}C NMR spectra. At −78 °C, the signal of the carbonyl group was split into *four* signals, two of which had the same intensity (Figure 3). This confirmed the formation of three diastereoisomers, as the two C_2 conformations account for a single carbonyl signal each, whereas the C_1 diastereoisomer has two different carbonyl signals with the same intensity. The same pattern was observed for the naphthyl carbon atom carrying the ester function as well as for the CH signal of the isopropyl units (Figure S3 in the Supporting Information)

On the basis of the presence of the three diastereoisomers, the methyl region of the ^{13}C NMR spectrum should display a total of eight signals because of the diastereotopicity of the methyl groups. A total of seven signals was observed, but two

dx.doi.org/10.1021/jo5005229 | J. Org. Chem. 2014, 79, 3725−3730

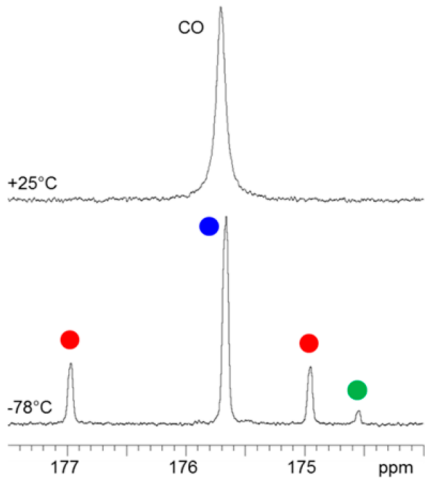

Figure 3. ^{13}C NMR spectra of the carbonyl signals of compound **7** (150.8 MHz in CD_2Cl_2). At −78 °C, the four signals ascribable to the three conformations are visible. Red dots indicate the signals of the C_1 conformation. Blue and green dots indicate the two C_2 conformations.

signals of the asymmetric conformation overlapped (Figure S3). A good indication of the relative ratio of the diastereoisomers as 64:31:5 was obtained from careful integration of the ^{13}C NMR signals at −78 °C, with the asymmetric conformation accounting for the 31% component.[17] When a diluted and carefully degassed CD_2Cl_2 sample was employed, the ^1H methyl region revealed the presence of two additional weak doublets partially overlapping with other peaks at −78 °C. The line shape simulation of the whole spectrum allowed a more accurate determination of the diastereomeric ratio as 63.5:33:3.5. Because the C_1 conformation is doubly degenerate, a statistical factor has to be added when evaluating the relative energies. Using the more populated C_2 conformation as a reference, ΔG° values were derived as 0.51 kcal/mol for the C_1 conformation and 1.10 kcal/mol for the less populated C_2 conformation.

Having established the presence of three conformational diastereoisomers due to the restricted rotation about the aryl−O bond, we pursued their assignment. The assignment of the C_1 conformation to the 33% conformer was straightforward because this conformation has four different methyl groups. On the contrary, because of the small energy differences, the structural assignment of the two C_2 conformations was not a trivial task. The assignment of the two C_2 conformers was based on the following three observations: (1) DFT calculations performed with the B3LYP or ωB97XD functional and the 6-311++G(2d,p) basis set suggested that the C_2-*out* geometry is the most stable conformation, followed by the C_1 conformer, while C_2-*in* was found to be the least stable isomer. (2) When a less polar solvent (toluene) was used instead of CD_2Cl_2,[18] the population of the less populated conformer increased. This suggests that the minor C_2 conformer has the C_2-*in* geometry, as it has a smaller dipole moment. (3) Comparison of chemical shift calculations at the GIAO-B3LYP/6-311++G(2d,p) level with the experimental NMR data are in agreement with the assignment of the more populated conformation to the C_2-*out* geometry (a full discussion of the conformational assignments is provided in the Supporting Information).

The experimental determination of the two rotational barriers was carried out by line shape simulation. The most informative analysis involved the ^1H NMR signals of the methyl groups because all of the expected lines were visible and the methyl signal is sensitive to both stereodynamic pathways. To simulate the two conformational pathways, one must consider that the rotation around the aryl−aryl bond not only causes enantiomerization but also exchanges the C_2-*out* and C_2-*in* conformations without populating the C_1 conformation. On the contrary, the aryl−oxygen rotation converts C_2-*in* into C_1 and then C_1 into C_2-*out* in a two-step mechanism involving the rotation of the second aryl−O bond. Within this section of the diastereomerization pathway, we have to consider that the two transition states involved are enantiomeric and that the rate constant for the second step of the pathway has to be halved to consider the reverse path leading to the starting point. In addition, each isopropyl group of the C_1 conformation has diastereotopic signals, and thus, in the forward direction the rate constant has to be furthermore halved to avoid the use of the same rate constant twice.

To assign the doublet pairs of the C_1 conformation, saturation transfer experiments (1D EXSY)[19] were recorded at −78 °C (Figure S7 in the Supporting Information). Upon saturation of the doublet at 1.27 ppm, the EXSY signal was observed with the doublet at 0.91 ppm, and the same signal was present when the doublet at 0.82 ppm was saturated. This means that the methyl at 0.91 ppm exchanges with the two doublets of the C_1 conformation at 1.27 and 0.91 ppm. Accordingly, the doublet at 0.76 ppm exchanges with the doublets at 0.94 and 1.02 ppm. Unfortunately, it was impossible to assign the doublets of the less populated conformation because they were partially overlapped and could not be selectively saturated.[20] However, the absence of any signal at 1.03 ppm in both of the acquired spectra strongly supports the hypothesis that the two doublets at 1.27 and 0.82 ppm exchange with the small doublet at 0.93 ppm. The above discussion is summarized in Scheme 2, in which the signals are numbered starting from the most deshielded signal for each conformation.

Scheme 2. (top) Numbering of the NMR Lines (^1H at 600 MHz, −78 °C in CD_2Cl_2); (bottom) Exchange Scheme and Related Rate Constants[a]

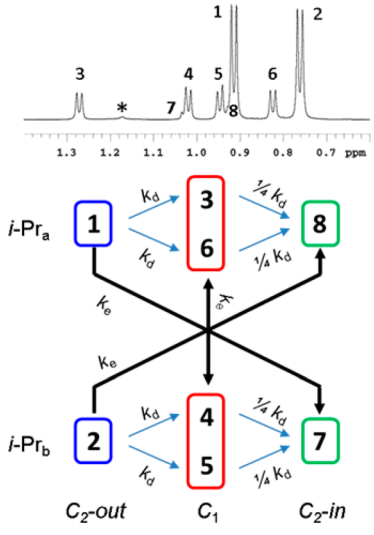

[a] k_d is the rate constant for diastereomerization due to aryl−O rotation, and k_e is the rate constant for enantiomerization due to aryl−aryl rotation.

dx.doi.org/10.1021/jo5005229 | J. Org. Chem. 2014, 79, 3725−3730

Line shape simulations were performed using a spin system composed of eight doublets with a 7.2 Hz coupling constant.[21] Very good line shape simulations could be obtained from −78 to −12 °C using only the diastereomerization rate constant k_d and the exchange pattern sketched in Scheme 2. At higher temperatures, the enantiomerization constant k_e had to be considered also. Figure 4 shows selected spectra and related

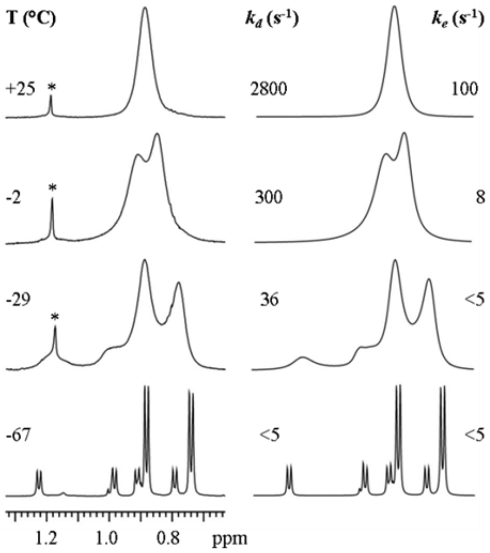

Figure 4. (left) Selected VT spectra of the ^{1}H NMR methyl signal of **7** (600 MHz in CD_2Cl_2). (right) Line shape simulations with the reported rate constants k_d and k_e. The singlet indicated by an asterisk is an impurity.

simulations at various temperatures.[22] The two free energy barriers derived from the rate constants by means of the Eyring equation were found to be 12.6 ± 0.2 and 14.9 ± 0.2 kcal/mol for the diastereomerization and enantiomerization processes, respectively.[23] The value of the diastereomerization barrier was independently measured by simulation of the ^{13}C NMR signals of the carbonyl and quaternary naphthyl carbons, which are split only when diastereoisomers are formed. In both cases, line shape simulations provided the same rate constants and the same diastereomerization barrier (12.6 ± 0.2 kcal/mol; see Figures S9 and S10 in the Supporting Information). Importantly, the experimental values are in good agreement with those provided by DFT calculations.

In summary, we have synthesized 2,2′-binaphthalene-1,1′-diol diisobutyrate (**7**) to provide insights into the dynamic stereochemistry of BINOL-derived tropos ligands, which have become increasingly useful in asymmetric catalysis and chirality sensing applications. Low-temperature NMR analysis revealed that **7** exists as a mixture of three rapidly interconverting conformations, denoted as C_1, C_2-*out*, and C_2-*in*. The ratio of these isomers was determined as 33:63.5:3.5 in CD_2Cl_2 at −78 °C. NMR line shape analysis showed that the activation Gibbs free energies for rotation about the axially chiral aryl−aryl bond and the two aryl−oxygen bonds are 14.9 and 12.6 kcal/mol, respectively. The experimentally obtained thermodynamic and kinetic data are in very good agreement with the results of DFT calculations. This study is expected to guide future catalysis and sensing developments.

EXPERIMENTAL SECTION

General Information. Commercially available reagents and solvents were used without further purification. NMR spectra were obtained at 400 MHz (^{1}H NMR) and 100.6 MHz (^{13}C NMR) in deuterated chloroform, unless noted otherwise. Chemical shifts are reported in parts per million relative to TMS. 2,2′-Binaphthalene-1,1′-diol (**6**) was prepared as described previously.[5e]

2,2′-Binaphthalene-1,1′-diol Diisobutyrate (7). 2,2′-Binaphthalene-1,1′-diol (50 mg, 0.18 mmol), and pyridine (85 μL, 1.05 mmol) were dissolved in 5 mL of dichloromethane, and the solution was cooled to 0 °C. Isobutyryl chloride (110 μL, 1.05 mmol) was added, and the mixture was allowed to warm to room temperature and stirred for 12 h. The reaction was quenched with 1 M HCl, and the resulting mixture was extracted with dichloromethane. The combined organic layers were dried over $MgSO_4$ and concentrated in vacuo. Purification by flash chromatography on silica gel (3:1 CH_2Cl_2/hexanes) afforded 60.4 mg (0.14 mmol, 81% yield) of a white solid. ^{1}H NMR: δ 0.98 (bs, 2H), 2.57 (septet, J = 6.7 Hz, 2H), 7.44 (d, J = 8.4 Hz, 2H), 7.52−7.54 (m, 4H), 7.78−7.81 (m, 4H), 7.89 (m, 2H). ^{13}C NMR: δ 18.6, 34.0, 121.5, 125.7, 126.5, 126.7, 127.2, 127.3, 128.0, 128.0, 134.2, 144.1, 174.9. Mp: 122−125 °C. HRMS (EI-double focusing, E/B): calcd for $C_{28}H_{26}O_4$, 426.18311; found, 426.18358.

Variable-Temperature NMR Spectroscopy. VT NMR spectra were recorded with a spectrometer operating at a field of 14.4 T (600 MHz for ^{1}H and 150.8 MHz for ^{13}C NMR). Low-temperature ^{1}H NMR spectra were acquired without spinning using a 5 mm dual direct probe with a 9000 Hz sweep width, 3.0 μs (30° tip angle) pulse width, 3 s acquisition time, and 1 s delay time. A shifted sine bell weighting function equal to the acquisition time (i.e., 3 s) was applied prior to the Fourier transformation. Usually 32 to 64 scans were collected. Low-temperature 150.8 MHz ^{13}C NMR spectra were acquired without spinning under proton-decoupling conditions with a 38 000 Hz sweep width, 4.5 μs (45° tip angle) pulse width, 1 s acquisition time, and 1 s delay time. A line broadening function of 1−2 Hz was applied before the Fourier transformation. Usually 256 to 1024 scans were collected. 1D EXSY spectra were recorded using the standard DPFGSE-NOE sequence[24] and a mixing time of 0.1 s. To selectively irradiate the desired signal, a 50 Hz-wide shaped pulse was calculated with a refocusing SNOB shape and a pulse width of 37 ms. Temperature calibrations were performed using a digital thermometer and a Cu/Ni thermocouple placed in an NMR tube filled with isopentane. The conditions were kept as equal as possible in all subsequent work. The uncertainty in temperature measurements can be estimated as ±1 °C. Line shape simulations were performed using a PC version of the QCPE DNMR6 program.[25] Electronic superimposition of the original and simulated spectra enabled the determination of the most reliable rate constant. The rate constants thus obtained at various temperatures afforded the free energy of activation ($\Delta G^{\ddagger}$) upon application of the Eyring equation. Within the experimental uncertainty due to the exact temperature determination, the activation energies were found to be invariant, thus implying a small entropy of activation ($\Delta S^{\ddagger}$).[26]

Calculations. The preliminary conformational searches were carried out with the molecular mechanics force field (MMFF) using Monte Carlo methods.[14] The most stable conformers thus identified were subsequently analyzed by DFT computations performed using Gaussian 09 with standard optimization parameters.[15] The calculations employed the B3LYP,[27] ωB97XD,[28] or M06-2X[29] functional and the 6-31G(d) or 6-311++G(2d,p) basis set. Harmonic vibrational frequencies were calculated for all of the stationary points. As revealed by the frequency analysis, imaginary frequencies were absent in all of the ground states, whereas one imaginary frequency was associated with each transition state. Visual inspection of the corresponding normal modes[30] validated the identification of the transition states.

ASSOCIATED CONTENT

Supporting Information

Full discussion of the conformational assignments, NMR spectra, and computational details. This material is available free of charge via the Internet at http://pubs.acs.org.

dx.doi.org/10.1021/jo5005229 | J. Org. Chem. 2014, 79, 3725−3730

AUTHOR INFORMATION

Corresponding Authors

*E-mail: andrea.mazzanti@unibo.it.
*E-mail: cw27@georgetown.edu.

Notes

The authors declare no competing financial interest.

ACKNOWLEDGMENTS

This material is partially based upon work supported by the NSF under CHE-1213019. The University of Bologna (RFO funds 2012) is also acknowledged.

REFERENCES

(1) (a) Shibasaki, M.; Matsunaga, S. *Chem. Soc. Rev.* **2006**, *35*, 269. (b) Brunel, J. M. *Chem. Rev.* **2007**, *107*, PR1.

(2) (a) Kyba, E. P.; Gokel, G. W.; de Jong, F.; Koga, K.; Sousa, L. R.; Siegel, M. G.; Kaplan, L.; Sogah, G. D. Y.; Cram, D. J. *J. Org. Chem.* **1977**, *42*, 4173. (b) Shimada, T.; Kina, A.; Hayashi, T. *J. Org. Chem.* **2003**, *68*, 6329. (c) Boyd, M. R.; Hallock, Y. F.; Cardellina, J. H., II; Manfredi, K. P.; Blunt, J. W.; McMahon, J. B.; Buckheit, R. W., Jr.; Bringmann, G.; Schäffer, M.; Cragg, G. M.; Thomas, D. W.; Jato, J. G.; Lough, A. *J. Med. Chem.* **1994**, *37*, 1740.

(3) (a) Desponds, O.; Schlosser, M. *Tetrahedron Lett.* **1996**, *37*, 47. (b) Tudor, M. D.; Becker, J. J.; White, P. S.; Gagné, M. R. *Organometallics* **2000**, *19*, 4376. (c) Maier, F.; Trapp, O. *Angew. Chem., Int. Ed.* **2012**, *51*, 2985.

(4) (a) Eelkema, R.; Feringa, B. L. *J. Am. Chem. Soc.* **2005**, *127*, 13480. (b) Eelkema, R.; Feringa, B. L. *Org. Lett.* **2006**, *8*, 1331.

(5) (a) Mizutani, T.; Tagaki, H.; Hara, O.; Horiguchi, T.; Ogoshi, H. *Tetrahedron Lett.* **1997**, *38*, 1991. (b) Ishii, Y.; Onda, Y.; Kubo, Y. *Tetrahedron Lett.* **2006**, *47*, 8221. (c) Etxebarria, J.; Degenbeck, H.; Felten, A.-S.; Serres, S.; Nieto, N.; Vidal-Ferran, A. *J. Org. Chem.* **2009**, *74*, 8794. (d) Anyika, M.; Gholami, H.; Ashtekar, K. D.; Acho, R.; Borhan, B. *J. Am. Chem. Soc.* **2014**, *136*, 550. (e) Bentley, K. B.; Nam, Y. G.; Murphy, J. M.; Wolf, C. *J. Am. Chem. Soc.* **2013**, *135*, 18052.

(6) (a) Mikami, K.; Matuskawa, S. *Nature* **1997**, *385*, 613. (b) Reetz, M. T.; Neugebauer, T. *Angew. Chem., Int. Ed.* **1999**, *38*, 179. (c) Mikami, K.; Terada, M.; Korenaga, T.; Matsumoto, Y.; Ueki, M.; Angelaud, R. *Angew. Chem., Int. Ed.* **2000**, *39*, 3532. (d) Walsh, P.; Lurain, A.; Balsells, J. *Chem. Rev.* **2003**, *103*, 3297. (e) Mikami, K.; Yamanaka, M. *Chem. Rev.* **2003**, *103*, 3369. (f) Reetz, M. T.; Li, X. *Angew. Chem., Int. Ed.* **2005**, *44*, 2959. (g) Aikawa, K.; Kojima, M.; Mikami, K. *Angew. Chem., Int. Ed.* **2009**, *48*, 6073. (h) Aikawa, K.; Mikami, K. *Chem. Commun.* **2012**, *48*, 11050. (i) Gajewy, J.; Gawronski, J.; Kwit, M. *Monatsh. Chem.* **2012**, *143*, 1045. (j) Ueki, M.; Matsumoto, Y.; Jodry, J.; Mikami, K. *Synlett* **2001**, 1889. (k) Chavarot, M.; Byrne, J.; Chavant, P.; Pardillos-Guindet, J.; Vallée, Y. *Tetrahedron: Asymmetry* **1998**, *9*, 3889. (l) Bolm, C.; Beckmann, O. *Chirality* **2000**, *12*, 523. (m) Gajewy, J.; Gawronski, J.; Kwit, M. *Eur. J. Org. Chem.* **2013**, 307. For a discussion of the stereochemical bias and reactivity of biphenyl 2,2′-dicarboxamides, see (n) Clayden, J.; Lund, A.; Youssef, L. H. *Org. Lett.* **2001**, *3*, 4133.

(7) Sahnoun, R.; Koseki, S.; Fujimura, Y. *J. Phys. Chem. A* **2006**, *110*, 2440.

(8) (a) *Dynamic Stereochemistry of Chiral Compounds*; Wolf, C., Ed.; RSC Publishing: Cambridge, U.K., 2008; pp 84−94. Also see: (b) Ruzziconi, R.; Spizzichino, S.; Lunazzi, L.; Mazzanti, A.; Schlosser, M. *Chem.—Eur. J.* **2009**, *15*, 2645. (c) Mazzanti, A.; Lunazzi, L.; Ruzziconi, R.; Spizzichino, S.; Schlosser, M. *Org. Biomol. Chem.* **2010**, *8*, 4463. (d) Lunazzi, L.; Mancinelli, M.; Mazzanti, A.; Lepri, S.; Ruzziconi, R.; Schlosser, M. *Org. Biomol. Chem.* **2012**, *10*, 1847.

(9) *Dynamic Stereochemistry of Chiral Compounds*; Wolf, C., Ed.; RSC Publishing: Cambridge, U.K., 2008; pp 94−99.

(10) Kessler, H.; Rieker, A.; Rundel, W. *Chem. Commun.* **1968**, 475.

(11) (a) Betson, M. S.; Clayden, J.; Worrall, C. P.; Peace, S. *Angew. Chem., Int. Ed.* **2006**, *45*, 5803. (b) Clayden, J.; Worrall, C. P.; Moran, W. J.; Helliwell, M. *Angew. Chem., Int. Ed.* **2008**, *47*, 3234.

(12) Siddall, T. H., III; Stewart, W. E.; Good, M. L. *Can. J. Chem.* **1967**, *45*, 1290.

(13) (a) Jennings, W. B. *Chem. Rev.* **1975**, *75*, 307. (b) Mislow, K.; Raban, M. *Top. Stereochem.* **1967**, *1*, 1. (c) Lunazzi, L.; Mazzanti, A.; Minzoni, M.; Anderson, J. E. *J. Org. Chem.* **2006**, *71*, 5474. (d) Casarini, D.; Lunazzi, L.; Mazzanti, A. *Eur. J. Org. Chem.* **2010**, 2035.

(14) MMFF conformational search as implemented in Titan 1.0.5: *Titan*, version 1.0.5; Wavefunction, Inc.: Irvine, CA, 2000.

(15) Frisch, M. J.; Trucks, G. W.; Schlegel, H. B.; Scuseria, G. E.; Robb, M. A.; Cheeseman, J. R.; Scalmani, G.; Barone, V.; Mennucci, B.; Petersson, G. A.; Nakatsuji, H.; Caricato, M.; Li, X.; Hratchian, H. P.; Izmaylov, A. F.; Bloino, J.; Zheng, G.; Sonnenberg, J. L.; Hada, M.; Ehara, M.; Toyota, K.; Fukuda, R.; Hasegawa, J.; Ishida, M.; Nakajima, T.; Honda, Y.; Kitao, O.; Nakai, H.; Vreven, T.; Montgomery, J. A., Jr.; Peralta, J. E.; Ogliaro, F.; Bearpark, M.; Heyd, J. J.; Brothers, E.; Kudin, K. N.; Staroverov, V. N.; Kobayashi, R.; Normand, J.; Raghavachari, K.; Rendell, A.; Burant, J. C.; Iyengar, S. S.; Tomasi, J.; Cossi, M.; Rega, N.; Millam, J. M.; Klene, M.; Knox, J. E.; Cross, J. B.; Bakken, V.; Adamo, C.; Jaramillo, J.; Gomperts, R.; Stratmann, R. E.; Yazyev, O.; Austin, A. J.; Cammi, R.; Pomelli, C.; Ochterski, J. W.; Martin, R. L.; Morokuma, K.; Zakrzewski, V. G.; Voth, G. A.; Salvador, P.; Dannenberg, J. J.; Dapprich, S.; Daniels, A. D.; Farkas, Ö.; Foresman, J. B.; Ortiz, J. V.; Cioslowski, J.; Fox, D. J. *Gaussian 09*, revision A.02; Gaussian, Inc.: Wallingford, CT, 2009.

(16) For reviews, see: (a) Exner, O. In *The Chemistry of Double-Bonded Functional Groups*; Patai, S., Ed.; Interscience: London, 1977; p l. (b) Jones, G. I. L.; Owen, N. L. *J. Mol. Struct.* **1973**, *18*, 1. (c) Eliel, E. L.; Wilen, S. H. *Stereochemistry of Organic Compounds*; Wiley-Interscience: New York, 1994; pp 618−621. Also see: (d) Pawar, D. M.; Khalil, A. A.; Hooks, D. R.; Collins, K.; Elliott, T.; Stafford, J.; Smith, S.; Noe, E. A. *J. Am. Chem. Soc.* **1998**, *120*, 2108. (e) Grindley, T. B. *Tetrahedron Lett.* **1982**, *23*, 1757.

(17) At low temperature, the relaxation times are shorter and the integration is more reliable. Moreover, within the same set of signals, the relaxation rates should be very similar.

(18) ε = 8.9 at 25°C and 15.0 at −81°C. See: Morgan, S. O.; Lowry, H. H. *J. Phys. Chem.* **1930**, *34*, 2385.

(19) (a) Hu, D. X.; Grice, P.; Ley, S. V. *J. Org. Chem.* **2012**, *77*, 5198. (b) Lunazzi, L.; Mazzanti, A.; Minzoni, M. *J. Org. Chem.* **2007**, *72*, 2501.

(20) The EXSY spectrum is much more effective when the less intense signal is saturated.

(21) The exact ratio of the three diastereoisomers was obtained by simulation of the −78 °C NMR spectrum, and the corresponding ΔG° values were determined at the same temperature. At higher temperatures, the populations were modified according to the Boltzmann equation to keep the free energy differences constant (this implies the assumption that $\Delta G^\circ = \Delta H^\circ$).

(22) Other spectra with simulations are reported in Figure S8 in the Supporting Information.

(23) As usually happens in conformational processes, the $\Delta G^{\ddagger}$ values derived from simulations were found to be almost invariant with temperature, thus implying a small entropy of activation ($\Delta S^{\ddagger}$).

(24) (a) Stonehouse, J.; Adell, P.; Keeler, J.; Shaka, A. J. *J. Am. Chem. Soc.* **1994**, *116*, 6037. (b) Stott, K.; Stonehouse, J.; Keeler, J.; Hwang, T. L.; Shaka, A. J. *J. Am. Chem. Soc.* **1995**, *117*, 4199. (c) Stott, K.; Keeler, J.; Van, Q. N.; Shaka, A. J. *J. Magn. Reson.* **1997**, *125*, 302. (d) Van, Q. N.; Smith, E. M.; Shaka, A. J. *J. Magn. Reson.* **1999**, *141*, 191.

(25) DNMR6: Calculation of NMR Spectra Subject to the Effects of Chemical Exchange (QCPE Program 633): Brown, J. H.; Bushweller, C. H. *QCPE Bull.* **1983**, *3*, 103. A PC version of the program is available on request from the authors.

(26) For a discussion about the evaluation of $\Delta S^{\ddagger}$ in conformational processes, see ref 13d. Also see: (a) Lunazzi, L.; Mancinelli, M.; Mazzanti, A. *J. Org. Chem.* **2007**, *72*, 5391. (b) Masson, E. *Org. Biomol. Chem.* **2013**, *11*, 2859.

(27) (a) Lee, C.; Yang, W.; Parr, R. G. *Phys. Rev. B* **1988**, *37*, 785. (b) Becke, A. D. *J. Chem. Phys.* **1993**, *98*, 5648. (c) Stephens, P. J.;

Devlin, F. J.; Chabalowski, C. F.; Frisch, M. J. *J. Phys. Chem.* **1994**, *98*, 11623.
(28) Chai, J.-D.; Head-Gordon, M. *Phys. Chem. Chem. Phys.* **2008**, *10*, 6615.
(29) Zhao, Y.; Truhlar, D. G. *Theor. Chem. Acc.* **2008**, *120*, 215.
(30) *GaussView*, version 5.0.9; Gaussian, Inc.: Wallingford, CT, 2009.

dx.doi.org/10.1021/jo5005229 | *J. Org. Chem.* 2014, 79, 3725−3730